

Self-Powered Electrical Stimulation for Enhancing Neural Differentiation of Mesenchymal Stem Cells on Graphene–Poly(3,4-ethylenedioxythiophene) Hybrid Microfibers

Weibo Guo,^{†,‡} Xiaodi Zhang,^{†,‡} Xin Yu,^{†,‡} Shu Wang,^{†,‡} Jichuan Qiu,[§] Wei Tang,[§] Linlin Li,^{*,†} Hong Liu,^{*,†,§} and Zhong Lin Wang^{*,†,||}

[†]Beijing Institute of Nanoenergy and Nanosystems, Chinese Academy of Sciences, National Center for Nanoscience and Technology (NCNST), Beijing 100083, People's Republic of China

[‡]University of Chinese Academy of Sciences, Beijing 100049, People's Republic of China

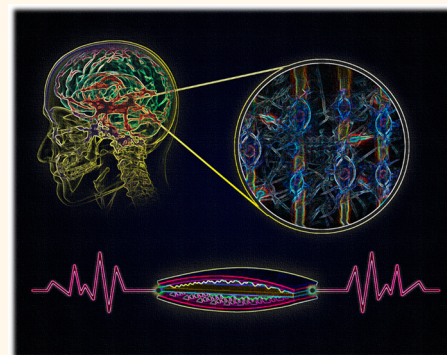
[§]State Key Laboratory of Crystal Materials, Shandong University, Jinan 250100, People's Republic of China

^{||}School of Materials Science and Engineering, Georgia Institute of Technology, Atlanta, Georgia 30332-0245, United States

Supporting Information

ABSTRACT: Engineered conductive scaffolds toward neural regeneration should have the ability to regulate mesenchymal stem cell (MSC) differentiation into neural lineage through an electrical stimulation-assisted culture process. In this work, a self-powered electrical stimulation-assisted neural differentiation system for MSCs was realized by combining a high effective triboelectric nanogenerator (TENG) to supply pulsed electric stimulation signals and a poly(3,4-ethylenedioxythiophene) (PEDOT)–reduced graphene oxide (rGO) hybrid microfiber (80 μm in diameter) as a scaffold. The conductive PEDOT endows the rGO–PEDOT hybrid microfiber with an enhanced electrical conductivity and maintains a good cytocompatibility. MSCs cultured on this highly conductive rGO–PEDOT hybrid microfiber possess enhanced proliferation ability and good neural differentiation tendency. Importantly, by inducing electric pulses generated by the TENG as the electrical stimulation signal, which are triggered by human walking steps, neural differentiation of MSCs is dramatically improved. This study illustrates the customizability of the rGO–PEDOT hybrid microfiber for neural tissue engineering scaffolding applications, underlines the potential of a self-powered TENG electrical stimulation system for accelerating MSC differentiation into neural cells without bio/chemical cues, and suggests the TENG's practical use as a wearable stimulation system to assist nerve regeneration for a walking person.

KEYWORDS: MSCs, neural differentiation, rGO–PEDOT microfiber, self-powered TENG, electrical stimulation



Neural tissue engineering (NTE) is considered to be one of the most promising approaches for regeneration of neural systems.¹ As is well-known, stem cell, scaffold, and bio/chemical/physical cues are the most important elements of NTE.² Mesenchymal stem cells (MSCs) are multipotent cells with the potential to differentiate into various cell types, including adipocytes, endothelial cells, osteoblasts and chondrocytes,³ cardiac muscle cells,⁴ hepatocytes,⁵ and neural cells.⁶ Because of the abundant sources and easy isolation, MSCs are considered to be one of the most important stem cell sources for neural regenerative medicine.⁷

MSCs in the natural state are not capable of differentiating into a particular neural lineage cell type but could be affected by some extrinsic factors such as chemical growth factors, extracellular matrix (ECM) components, as well as the electrical or mechanical cues from their microenvironment for neural commitment.⁸ So, engineered NTE scaffolds with the appropriate geometry as well as excellent biological and ideal

Received: January 10, 2016

Accepted: May 4, 2016

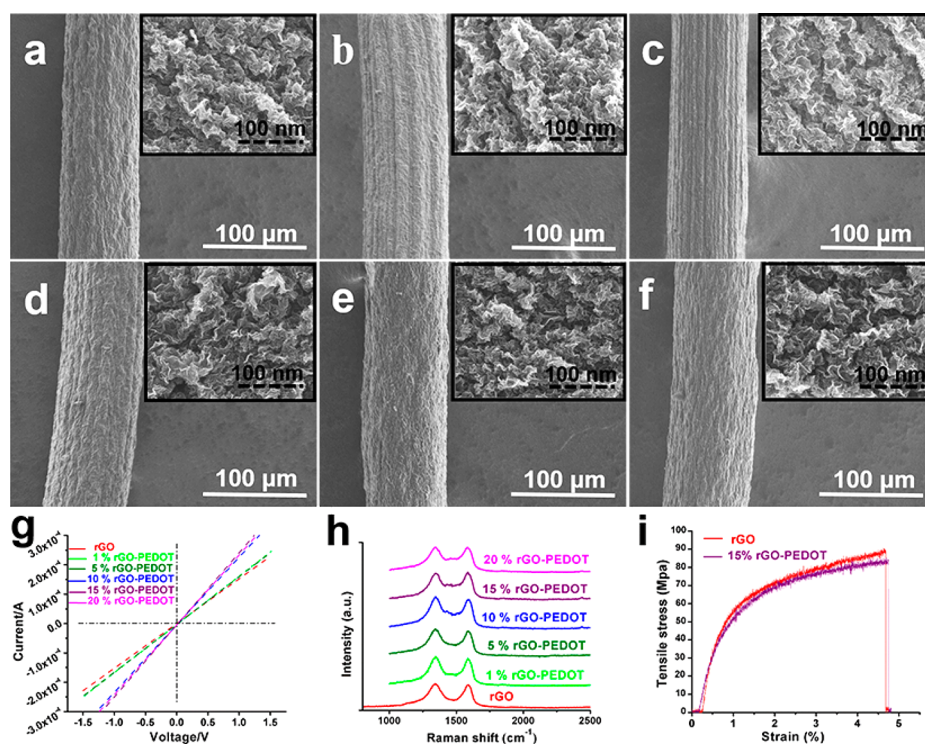


Figure 1. SEM images of the microfibers. (a–f) rGO or rGO–PEDOT microfibers made from 8 mg/mL GO suspension containing 0, 1, 5, 10, 15, and 20 vol % of 50 $\mu\text{g}/\text{mL}$ PEDOT solution, respectively. The insets are high-resolution SEM images of the surface morphologies of the microfibers. (g) I – V curves of the hybrid microfibers with different PEDOT content. (h) Raman spectra of the microfibers with different PEDOT content. (i) Stress–strain curves of experimental rGO microfiber (red) and 15% rGO–PEDOT microfiber (blue).

physical and electrical properties have been desired for neural differentiation.⁹

Due to its excellent mechanical stability, electrical conductivity, biocompatibility, and biodegradation ability, graphene has great potential for biomedical applications in the fields of scaffolds for tissue engineering,^{10,11} components of implant devices,¹² and substrates for differentiation of stem cells,¹³ but it is difficult to produce.¹⁴ Graphene oxide (GO) consists of graphene sheets that are chemically functionalized with hydroxyl and carboxyl groups and possesses excellent plasticity. So, GO could be used to fabricate nanostructured bulk materials with different morphology through *in situ* reduction reactions.¹⁵ Even the extended π -conjugation of the graphene surface is largely recovered after reduction, and the electrical conductivity of the rGO is still much lower than that of pristine graphene due to the remaining oxygen-containing functional groups that could disrupt the electronic structure of graphene.¹⁵ Nevertheless, GO could be an ideal material for manufacture of graphene-based biomaterials.¹⁶ To improve the conductivity of rGO-based materials, chemical modification of rGO with some conductive organic materials may be one of the most promising approaches. Some biocompatible conducting polymers have attracted enormous attention in neural therapies, including recording, stimulating neural activity, regeneration of neural tissue, and the delivery of bioactive molecules for mediating device–tissue interactions because of their high conductivity and good processing ability.¹⁷ One of the most promising candidates for biomedical applications, especially for neural therapy applications, is poly(3,4-ethylenedioxythiophene) (PEDOT).¹⁸ Although PEDOT is a good candidate for preparation of the scaffold of neural tissue regeneration, it has intrinsic disadvantages, such as difficulty forming special

shaped porous structures due to its lack of free functional groups and great difficulty degrading *in vitro*.¹⁹ During the formation process of the hybrid nanostructures, the carboxylic acid groups of GO nanosheets with negative charges provide a large number of sites to incorporate PEDOT nanoparticles,²⁰ so it is expected that integrating the good bioactivity of rGO and high conductivity of PEDOT to form a highly conductive biocompatible rGO–PEDOT hybrid biomaterial is a good approach for preparation of the NTE scaffold.

However, the MSCs' neural differentiation enhanced by the improvement of the scaffolds' electric conductivity is very limited. Recently, as a physical cue, pulse electrical stimulation has been proven to be an effective way to enhance the nerve regeneration process by using a conductive scaffold as media.^{21,22} In a practical pulse electricity-assisted nerve regeneration process, an attachable and portable electrical stimulation system is essential as a power supplier.²³ At present, almost all electrical stimulation for clinical or experimental nerve regeneration is supplied by traditional electrical stimulators, which are expensive, not portable, and need an external power supply. Moreover, a normal electrical stimulator connected to a 220 V power source attached on the body for nerve regeneration is uncomfortable, inconvenient, and unsafe. Battery-like power suppliers also face some problems, such as low-voltage, short lasting time, and difficulty being attached to the animal models of patients. Therefore, a long-lasting and portable self-powered electrical stimulation system with small size and small weight is urgently required for nerve regeneration devices. The invention of the triboelectric nanogenerator (TENG) has provided an effective approach for mechanical-to-electrical energy transduction.²⁴ The working principle of the TENG is based on the combination of contact

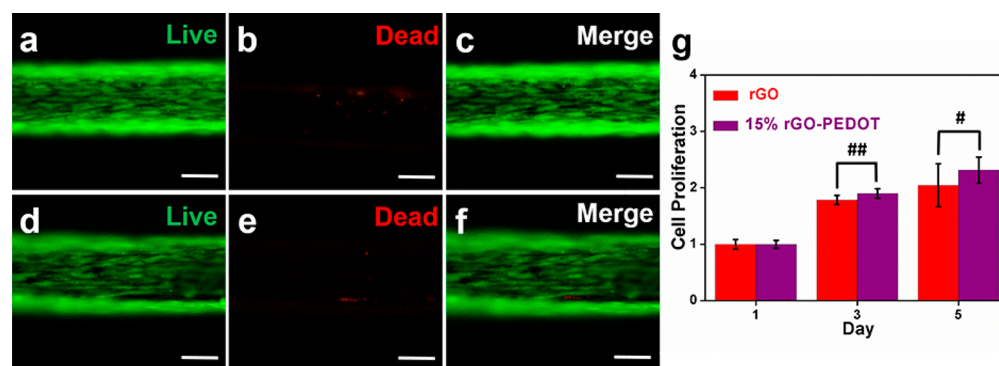


Figure 2. Cell viability assay of MSCs on the rGO microfiber (a–c) and 15% rGO–PEDOT hybrid microfiber (d–f) after 3 days of normal culture assessed by the live/dead assay; dead cells were stained with red, and live cells were stained with green (scale bar = 50 μm). (g) Proliferation of MSCs cultured on rGO microfibers and 15% rGO–PEDOT hybrid microfibers in 5 days was measured by a CCK-8 assay ($^{\#}p \leq 0.05$, $^{\#\#}p \leq 0.01$, $n = 3$).

electrification and electrostatic induction, and it has been systematically studied by Wang's group.²⁵ Recently, TENG-based devices for potential applications in photocatalytic,²⁶ air purification,²⁷ implantable pacemaker power source systems,²⁸ and wearable cloths²⁹ have been investigated and have shown numerous advantages. Combination of TENG and a highly conductive scaffold to build a self-powered electrical stimulating system for neural differentiation should be a practical way toward highly effective tissue regeneration.

In this work, a highly electrically conductive rGO–PEDOT hybrid microfiber with a diameter of 80 μm was prepared as the neural scaffold, and a step-driven TENG with outputs of 250 V and 30 μA was built as the electrical simulation power source. A step-driven self-powered neural differentiation system was integrated by combining the hybrid microfiber and the TENG. The rGO–PEDOT hybrid microfiber can not only enhance the proliferation of MSCs but also function as a medium for step-driven TENG pulse electrical simulation signals, which can induce MSCs to differentiate into neural cells. The study realizes an enhancement of MSC neural differentiation on the rGO–PEDOT hybrid microfiber under TENG-driven electrical pulse simulation. This work shows a significant potential application of a self-powered wearable TENG electrical stimulation system for the assistance of nerve regeneration.

RESULTS AND DISCUSSION

The morphologies and microstructures of as-prepared microfibers, which are synthesized by a capillary hydrothermal method (Figure S2) with GO as the raw material, are shown in Figure 1. Figure 1a–f shows scanning electron microscopy (SEM) images of rGO and rGO–PEDOT microfibers made from 8 mg/mL GO solution containing PEDOT solution with a volume content of 0, 1, 5, 10, 15, and 20%, respectively. All microfibers are of uniform straight morphology with a diameter of about 80 μm . From the high-resolution SEM images in the insets of Figure 1a–f, we can see that the surfaces of all the microfibers with different contents of PEDOT have similar three-dimensional (3D) porous nanostructures, with a pore size of approximately 50 nm without any obvious difference. The results suggest that the addition of PEDOT nanoparticles would not affect the morphology and nanostructure of the rGO microfiber. From Supporting Information S1, we find that the rGO–PEDOT nanostructures were formed by PEDOT nanoparticles (50 nm) (Figure S1b) uniformly wrapped

under rGO sheets, which does not affect the morphology of rGO and the reunion ability of GO sheets (Figure S1a) during the hydrothermal process. The electrical conductive performance of the microfibers was tested, and the digital picture of electrodes of the samples is shown in Figure S3. As is shown in the I – V curves (Figure 1g), the calculated electrical conductivity of the as-prepared rGO microfiber is ~ 1.51 S/cm, and the electrical conductivity of 1, 5, 10, 15, and 20% rGO–PEDOT hybrid microfibers is ~ 1.68 , ~ 1.69 , ~ 2.22 , ~ 2.52 , and ~ 2.41 S/cm, respectively. The results suggest that the content of PEDOT in the rGO–PEDOT hybrid microfibers can significantly affect the conductivity of the rGO microfiber, and rGO–PEDOT hybrid microfibers with volume content of 15% PEDOT have the highest conductivity, which is chosen for the following bioexperiment. The crystalline structures of the graphene nanosheets of the rGO microfiber and rGO–PEDOT hybrid microfibers were assessed by Raman spectroscopy. As shown in Figure 1h, the D-band (located at 1350 cm^{-1}) and G-band (located at 1590 cm^{-1}) can be observed in all microfibers, but a bare PEDOT Raman shift is not shown (Figure S4a). The ratio of D-band to G-band provides a useful probe of the relative degree of alignment, while all of the ratios are about 1:1 for the microfibers,³⁰ indicating that the alignment of graphene nanosheets is not affected by the mixture of PEDOT. From the Fourier transform infrared (FTIR) spectra (Figure S4b), the GO characteristic peaks including O–H (3300 and 1418 cm^{-1}), C=O (1742 cm^{-1}), C–OH (1367 cm^{-1}), and C–O (1067 cm^{-1}) as well as the PEDOT characteristic peak of ethylenedioxy located at 1140 cm^{-1} were observed. The characteristic peaks of oxygen-containing groups were weakened on the rGO FTIR spectrum curve, but there were still many O–H and C=O groups. The rGO–PEDOT curve is similar to the rGO spectrum curve but presents the characteristic peak of ethylenedioxy, which demonstrates the presence of PEDOT. As described in S5, due to the higher content of oxygen-containing groups,^{31–34} a 15% rGO–PEDOT hybrid microfiber has a protein adsorption ability better than that of the rGO microfiber. The biodegradation behaviors of scaffolds are highly important for their potential use in tissue engineering.³⁵ Because the microfibers were obtained by the hydrothermal process without any chemical reducing agent, the surface nanopore-structured, oxygen-containing-group-rich and low graphitization extent of the rGO microfiber and 15% rGO–PEDOT hybrid microfiber could be biodegraded by horseradish peroxidase (HRP) in the

presence of H_2O_2 .^{36,37} The SEM, FTIR, Raman spectra, and the percentage of residual mass of the rGO microfiber and the 15% rGO–PEDOT hybrid microfiber (Figure S6) indicate that the microfibers have similar biodegradability speed (see details in Figure S6). The tensile strength of the rGO microfiber is about 86 MPa and about 84 MPa for the 15% rGO–PEDOT hybrid microfiber at room temperature (Figure 1i), indicating that the microfibers possess good mechanical properties and that the mixture of PEDOT does not significantly affect the mechanical property of the microfibers.

The above results illustrate that the as-prepared microfibers are uniform nanoporous surface structured. The electrical conductivities of the rGO microfiber can be significantly improved by compositing with PEDOT. The rGO–PEDOT hybrid microfiber doped by PEDOT with a volume content of 15% and possessing the best conductivity was chosen for the following bioexperiment. Above all, the morphologies, relative degrees of alignment, biodegradability, and mechanical properties of the 15% rGO–PEDOT hybrid microfibers were not affected by the addition of PEDOT, but rGO–PEDOT microfibers have a protein adsorption ability better than that of the rGO microfiber.

The flow cytometry purity analysis of the isolated MSCs indicates that the cells' purity was greater than 90%, as illustrated in Figure S7. To investigate the response of MSCs to the rGO microfiber and 15% rGO–PEDOT hybrid microfiber, third-passage MSCs were seeded on the two microfibers at a density of 5×10^4 per dish (24-well plate). Live/dead cell staining was assayed after the MSCs were seeded on the microfibers for 72 h under normal culture conditions, where dead cells were stained with red and live cells were stained with green. The fluorescent images of the live/dead-stained MSCs on the rGO microfiber (Figure 2a–c) and the 15% rGO–PEDOT hybrid microfiber (Figure 2d–f) illustrate that more than 99% of the seeded cells survived on the microfibers, and there is almost no difference in the cell viability between the two microfibers. The proliferation of MSCs on the two microfibers was also assessed after cultivation of the cells for 1, 3, and 5 days. As depicted in Figure 2g, the proliferation rate of the MSCs on the 15% rGO–PEDOT hybrid microfiber was somewhat higher than that on the pure rGO microfiber. The cell quantity increased rapidly on both scaffolds after 3 days, and the cells on the 15% rGO–PEDOT hybrid microfiber had a higher proliferation rate. After 5 days, the cell quantities on the 15% rGO–PEDOT hybrid microfibers was about ~ 1.16 -fold higher than that on the rGO microfibers. It is mainly because of the better protein adsorption ability of the 15% rGO–PEDOT hybrid microfibers, which is a benefit for the cell adhesion.³⁴ The results suggest that both the rGO microfiber and the 15% rGO–PEDOT hybrid microfiber have excellent cytocompatibility, and the addition of PEDOT in rGO induces a better platform for MSC proliferation.

The morphologies of the MSCs on the microfibers after 3 days under normal culture conditions were also observed *via* actin cytoskeleton staining on the rGO microfiber (Figure 3a–c) and the 15% rGO–PEDOT hybrid microfiber (Figure 3d–f). The cells that covered the microfibers with a typical geometry structure had a better cell adhesion status than that cultured on the smooth graphene film (shown in S8), and the cells were aligned straight on the microfibers, which indicated that both the rGO microfiber and the 15% rGO–PEDOT hybrid microfiber with nanoporous topographies were suitable for the adhesion of MSCs without laminin or polylysine

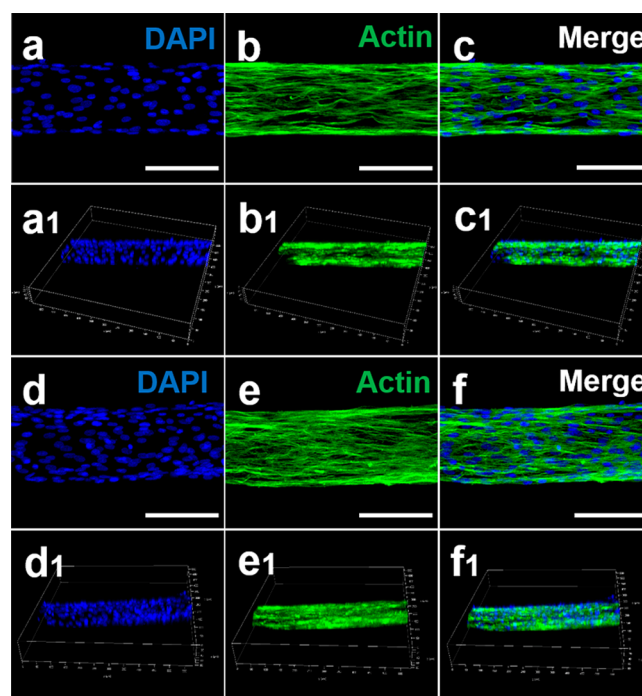


Figure 3. Two-dimensional structures of CLSM fluorescence morphologies of the actin cytoskeleton of the MSCs cultured on the rGO microfiber (a–c) and 15% rGO–PEDOT hybrid microfiber (d–f) after normal culture for 3 days. The actin filaments of the cells were stained with AlexaFluor 488–phalloidin (green), and the nuclei were stained with DAPI (blue) (scale bar = $100 \mu\text{m}$). Three-dimensional structures of the CLSM fluorescence morphologies of the MSC actin filaments on the rGO microfiber (a1–c1) and 15% rGO/PEDOT hybrid microfiber (d1–f1) reveal the 3D cell culture framework of the microfiber.

coating. Movie S1, Movie S2, and their 3D fluorescence images of the rGO microfiber (Figure 3a1–c1) and the 15% rGO–PEDOT hybrid microfiber (Figure 3d1–f1) also suggest that MSCs spread uniformly around the two different microfibers. Additionally, from the quantity of nuclei (DAPI, blue), the quantity of cells on the 15% rGO–PEDOT hybrid microfiber was more noticeable than that on the rGO microfiber. Along with the CCK-8 assay, it means that the cell adhesion and proliferation are more active on the 15% rGO–PEDOT microfiber.

The physical property of biomaterials has been proven to be one of the most important considerations for designing high-performance tissue engineering scaffolds because the physical property of the materials can affect the adhesion, proliferation, and even differentiation of stem cells.³⁸ The above results show that the rGO microfiber and 15% rGO–PEDOT microfiber have excellent cytocompatibilities for the MSCs. It seems that the addition of PEDOT nanoparticles in rGO fibers can promote the proliferation of MSCs because the rGO–PEDOT hybrid microfiber possibly provides a mitogenic cue,²¹ either directly or as a consequence of improving the adsorption of proteins due to the cross-linking of GO and PEDOT. As expected, the 15% rGO–PEDOT should possess enhanced neural differentiation ability for MSCs due to its much higher conductivity.

The TENG has a layered structure with two substrates, as shown schematically in Figure 4a. Due to its decent strength, light weight, and low cost, poly(methyl methacrylate) (PMMA)

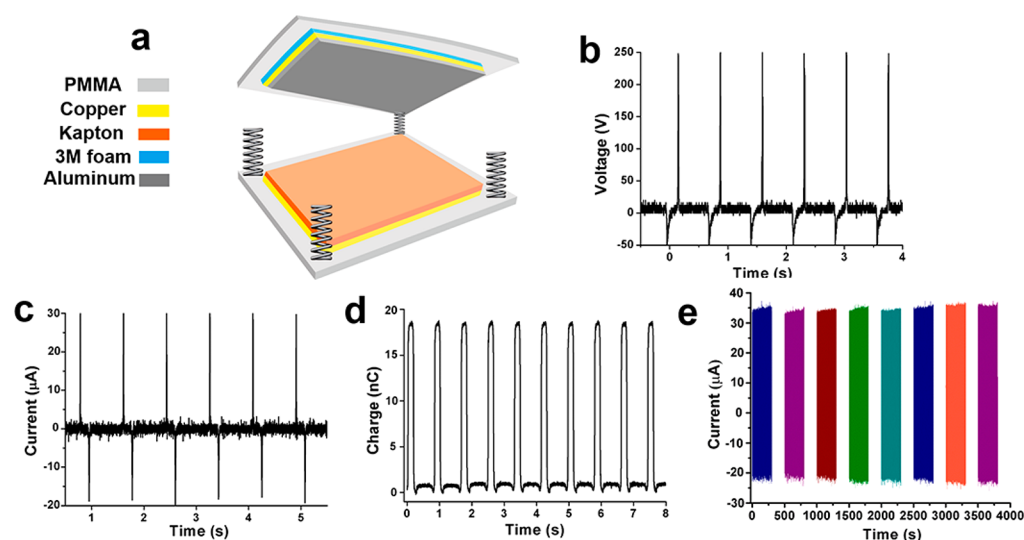


Figure 4. Structural design and characterization of the TENG. (a) Schematic illustration of the springs installed on the TENG; (b) induced voltage, (c) current, and (d) transferred charge of the TENG under a periodic external mechanical force. (e) Stability experiment of the TENG current output in 4000 s (about 3360 pulses).

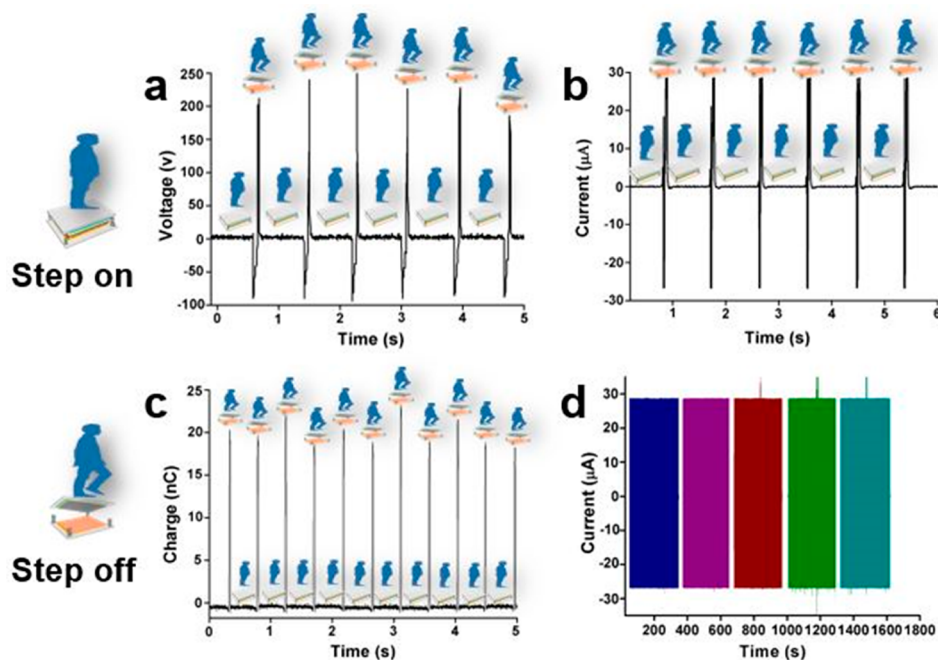


Figure 5. TENG can work with human motions, and the typical (a) induced voltage, (b) current, and (c) transferred charge of TENG is driven by walking steps. (d) Stability of the TENG current output in 1500 s (about 4500 pulses).

was chosen as the substrate material. The two substrates were connected by four springs installed at the corners. On the lower side, a layer of copper film was laminated between a layer of Kapton film, and the PMMA substrate was prepared. The contact electrode on the other side, a 2 mm film of 3 M foam as the stress buffer layer, was fixed on the PMMA substrate, which can help to maintain the stability of the TENG. Next, a copper film layer and an aluminum film layer were smoothly pasted on the 3 M layer in sequence. The photograph of the as-fabricated TENG is exhibited in Figure S9.

The electric energy generation process can be explained by the coupling between triboelectric and electrostatic effects.³⁹ The electric characterizations were assessed by a Keithley 2400 system electrometer and a SRS70 low-noise current amplifier

from Stanford Research System. The results of induced voltage, current, and transferred charge are shown in Figure 4b–d. The TENG gave an induced voltage of about 300 V; the short-circuit current reached a peak value of +30 and $-20 \mu\text{A}$, and the transferred charge during one circuit was around 18 nC.

The TENG was triggered by a motor with a displacement of $\pm 0.5 \text{ mm}$ and a frequency of 84 times per minute for the assessment of its output stability. The current was measured for a continuous 4000 s, and the output current pulses in 300 s were recorded after a 200 s interval. In Figure 4e, about 3360 pulses were recorded, and the short-circuit currents could almost reach the peak value of $35 \mu\text{A}$. After 3360 pulses, the output current did not show any significant decay, which demonstrates that the TENG has good electrical output

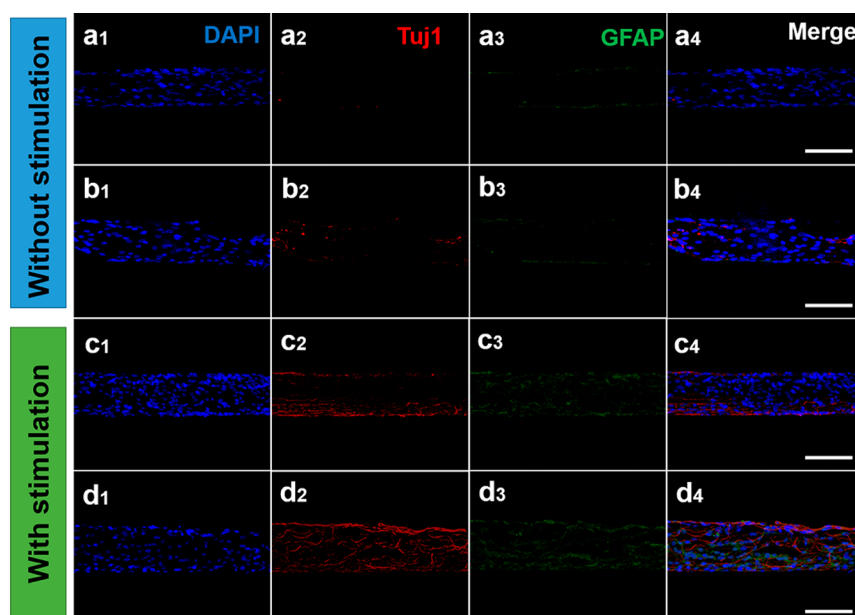


Figure 6. Cells were immunostained with (1) DAPI (blue) for the nucleus and neural-specific antibodies (2) Tuj1 (red, cy3), (3) GFAP (green, FITC) after being cultured under stimulation culturing conditions without TENG electrical stimulation (a,b) or with human-motion-driven TENG electrical stimulation (c,d) for 21 days on rGO microfiber (a,c) and 15% rGO–PEDOT hybrid microfiber (b,d). (Right) Merged fluorescence images (scale bar = 100 μm).

stability. Because the separation of the contact electrode and Kapton is caused by the restoring force of the springs, which maintains a fixed distance between them, the TENG could provide a stable electrical output. Therefore, the electrical output of the TENG can provide a stable power source for electrical pulse stimulation without any addition of circuit to change the output voltage or current.

Some previous studies showed that the TENGs can be triggered by some commonly available mechanical sources, such as wind, waves, vehicle wheels, and even heart beats.⁴⁰ In this study, investigated the electrical signals of the TENG that are driven by human motions. The output of the TENG triggered by walking is shown in Figure 5. The results of induced voltage, current, and transferred charge are shown in Figure 5a–c. The TENG gives a walking-induced voltage of about 300 V (even as high as 340 V); the short-circuit current reached a peak value of +30 and $-28 \mu\text{A}$, and the transferred charge during one circuit was around 20 nC. The current was measured for a continuous 1500 s with a frequency of three times per second, and the output current pulses in 300 s were recorded after a 50 s interval. In Figure 5d, about 4500 pulses were recorded, and after 4500 pulses, the output current did not show any significant decay, which demonstrates that the TENG has good electrical output stability under human motions. The results illustrate that the TENG's electrical signals are slightly higher than that from the motor-driven TENG, which should be caused by a larger contact force from human motions.⁴⁰ In similar studies on the electric pulse simulation of MSCs for neural differentiation, the stimulation threshold was 20–50 μA , so the TENG with a current output of about 30 μA is suitable for cellular electrical stimulation applications.⁴¹

Two groups of microfibers, rGO microfibers and 15% rGO–PEDOT microfibers, were used to assess the effect of human walking motion on the TENG-based electric pulse simulation of neural differentiation of MSCs. Experiments for the

assessment of *in vitro* differentiation of MSCs were divided into four groups: two reference groups of rGO microfibers and 15% rGO–PEDOT microfibers without TENG stimulation treatment and another two treatment groups of rGO microfibers and 15% rGO–PEDOT microfiber TENGs with stimulation groups (3000 pulses/day). The MSCs in the stimulation groups were cultured in a self-made culture plate to realize pulsed electrical stimulation (shown in Figure S10). Before electrical stimulation treatment, all of the cells were cultured under normal culture conditions for 3 days to ensure that the stem cells were well-attached to the microfibers. After cell attachment, the reference groups were kept in the same conditions for another 21 days, and the simulation groups were processed with walking-driven TENG stimulation for another 21 days.

As is shown in the DAPI-stained images of the MSCs cultured on the rGO microfiber (Figure 6a1,c1) and the 15% rGO–PEDOT hybrid microfiber without electrical stimulation (Figure 6b1,d1) after 21 days, the distribution and density of cells do not have obvious differences compared with those on the two microfibers for 3 days (Figure 3). To evaluate the effects of the intrinsic properties of materials and the TENG stimulation on the neural differentiation of MSCs, the expression of two neural special markers (Tuj1 for neuron cells and GFAP for glial cells) was assessed by immunostaining. Without TENG electrical stimulation, the cells on the rGO microfiber have almost no Tuj1 expression (Figure 6a2), with a low Tuj1 expression on the 15% rGO–PEDOT hybrid microfiber (Figure 6b2). However, GFAP expressions on the rGO microfiber (Figure 6a3) and 15% rGO–PEDOT hybrid microfibers (Figure 6a3) have no obvious difference. The results proved that the addition of PEDOT could enhance a certain degree of Tuj1 expression, which means that the 15% rGO–PEDOT hybrid microfiber could have an enhancement for neural differentiation of MSCs stronger than that of glial differentiation of MSCs.

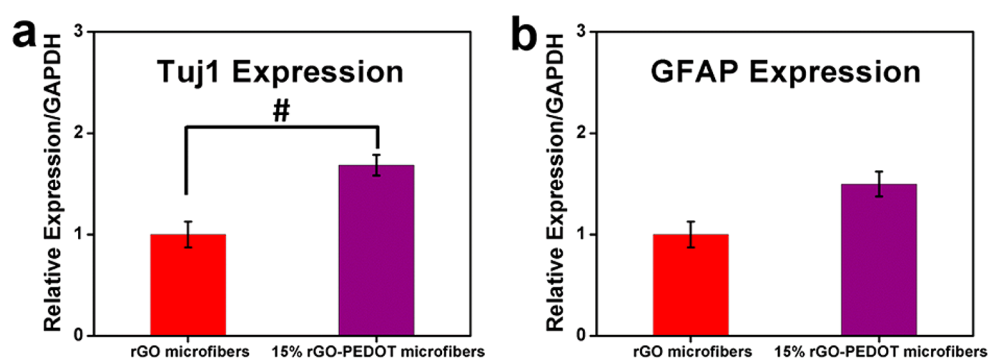


Figure 7. qPCR analysis of the cell expression levels of neural-specific genes of Tuj1 (a) and GFAP (b) on the rGO microfibers and 15% rGO–PEDOT hybrid microfibers; cells were stimulated by the human-walking-driven TENG for 21 days ($^{\#}p \leq 0.05$, $^{\#\#}p \leq 0.01$, $n = 3$).

The excellent cell adhesion and connection on the microfibers could ensure the cell-to-cell information exchange. The chemical stabilities of graphene and PEDOT support that no chemical change occurs with the charge injection. With electrical pulse stimulation from human-walking-driven TENGs for 21 days, as is observed from DAPI staining images of the rGO microfiber (Figure 6c1) and the 15% rGO–PEDOT microfiber (Figure 6d1), the cell viability is not influenced by the electrical stimulation, but there are obvious differences between Tuj1 and GFAP expressions on the two microfibers. Compared with that on rGO microfibers, the Tuj1 and GFAP expression cells on the 15% rGO–PEDOT microfiber are both significantly enhanced. It can be found that Tuj1 (Figure 6c2) and GFAP (Figure 6c3) expressions of cells on the rGO microfiber are less than those on the 15% rGO–PEDOT hybrid microfiber (Figure 6d2,d3). Figure S11 suggests that the stimulation effect of the human-motion-driven TENG is not worse than that of the linear motor-triggered TENG.

To further confirm the result of immunostaining, the gene expression levels of Tuj1 and GFAP were evaluated. As shown in Figure 7, the qPCR result reveals that the expression of Tuj1 on the 15% rGO–PEDOT hybrid microfiber was enhanced by ~ 1.68 -fold over that on the rGO microfiber. Meanwhile, there was also a significant difference in GFAP expression, which was approximately ~ 1.5 -fold higher for the cells on the 15% rGO–PEDOT hybrid microfiber. With regard to the results, the better electrical conductivity of the 15% rGO–PEDOT hybrid microfiber makes the current transmission stronger, and the stronger charge injection increases neural proteins and gene expressions.

The flexibility, stiffness, dimensions, topographical, and electrical properties of the scaffolds could induce biological effects that regulate the fate of stem cells.⁴² For the regenerative therapies in the neural system, functional neuron cells are often the therapeutic target cells.⁴³ Neural cells are electroactive ones, and a bioelectronic interface can affect neural cell behaviors. The rGO–PEDOT hybrid microfiber is a better charge transport platform for electrical cellular interfacing applications to regulate nerve cell behaviors, which leads to a more active Tuj1 expression of MSCs. These results indicate that the TENG stimulation could promote MSC neural differentiation, especially on the rGO–PEDOT hybrid microfiber. It clearly implies that the rGO–PEDOT hybrid microfiber can work better as a conductive scaffold for electrical stimulation applications to the cells, and the as-fabricated TENG is suitable as a self-powered electrical stimulator.

Additionally, it has been demonstrated that the TENG could work well after being implanted into small animal bodies, but it would have a strict limitation in the TENG size, which would limit the output of the TENG.²⁸ Wearable TENGs seem to be more appropriate for the treatment-assisted application for nerve regeneration from electrical stimulation devices. It is well-known that walking is one of the best recovery exercises for the patients with neurological diseases. The as-fabricated light, size small, low cost, self-powered, and output-stable springs installed in the TENG might make them promising candidates for wearable neural electrical stimulation devices.

CONCLUSION

In summary, we introduce a promising strategy for combining a low-cost, small-sized, and long-lasting self-powered TENG and electroconductivity-improved rGO–PEDOT hybrid microfibers to build a self-powered electrical stimulation system for stem cell neural differentiation. A human-motion-driven self-powered TENG with an output of 300 V and 30 μ A was built as the electrical stimulation power source, and an electrical conductivity improved, mechanically strong, cytocompatible, and biodegradable rGO–PEDOT hybrid microfiber was prepared as the neural scaffold. The human-motion-driven self-powered TENG provided by electrical stimulation signals through the rGO–PEDOT hybrid microfibers can induce MSC differentiation into neural cells with neural-specific proteins and gene expressions greater than those of the rGO microfibers. This work not only provides a promising conductive NTE scaffold but also shows a significant potential application of a self-powered, wearable, electrical stimulation TENG system to assist nerve regeneration.

METHODS

Preparation of Graphene Oxide. GO powder was obtained by the modified Hummers' method. Graphite powder was pretreated with concentrated H_2SO_4 , $\text{K}_2\text{S}_2\text{O}_8$, and P_2O_5 . Second, the pretreated graphite powder was oxidized with concentrated H_2SO_4 and KMnO_4 by the traditional Hummers' method.⁴⁴ Then, the GO powder was dispersed in deionized water, and the remaining salt impurities were removed by dialysis for 7 days, exchanged with deionized water daily, to finally obtain the GO solution with a certain concentration of 8 mg/mL.

Preparation of the rGO Microfiber and the rGO–PEDOT Hybrid Microfiber. The microfibers were produced by a modified capillary hydrothermal method, which is similar to the method in ref 30. The GO water suspension with a concentration of 8 mg/mL and a solution mixed with 8 mg/mL of GO and 50 μ g/mL of PEDOT (Sigma) with volume fractions of 1, 5, 10, 15, and 20% were injected into a glass pipeline with a 0.8 mm inner diameter and 100 cm length.

The glass pipeline was sealed up on both ends (Figure S3), heated, and maintained at a temperature at 220 °C for 6 h. The rGO–PEDOT hybrid microfibers synthesized from the solution with volume fractions of 1, 5, 10, 15, and 20% are abbreviated as 1% rGO–PEDOT microfiber, 5% rGO–PEDOT microfiber, 10% rGO–PEDOT microfiber, 15% rGO–PEDOT microfiber, and 20% rGO–PEDOT microfiber, respectively. The morphology of rGO microfiber and rGO–PEDOT microfiber inherits the shape of the pipeline cavity and displays a fiber-like material with very small diameter after hydrothermal treatment and drying, which is discussed in Supporting Information S2.

Characterization of the Samples. The morphology of the samples was characterized with SEM (SU8020, Hitachi, Japan). The room temperature electrical property was measured by a semiconductor characterization system (Keithley 4200-SCS). A Dilor XY microspectrometer with a 532 nm laser excitation was used to record the Raman spectra of the samples. The FTIR spectrum was assessed by a Bruker Vertex 80v spectrometer. The tensile test was performed by an Instron material testing system (Instron 3365/series IX/s).

Cell Culture. Adult rats (Wistar, male, 4 weeks old) used for experiment were purchased from Vital River Company, and our procedures for handling the animals strictly followed the “Beijing Administration Rule of Laboratory Animals” and the national standards “Laboratory Animal Requirements of Environment and Housing Facilities (GB 14925–2001)”. MSCs were isolated from rats as previously described.³⁰ Under normal culture conditions, the cells were cultured in primary medium containing low glucose (1.0 g/L) Dulbecco’s modified Eagle’s medium (L-DMEM, Gibco) supplemented with 10% fetal bovine serum (FBS, Gibco), 1% penicillin–streptomycin (Gibco), and 4 ng/mL basic fibroblast growth factor (bFGF). MSCs at the third passage were used for all of the following experiments.

Electrical Stimulation of MSCs on the Microfibers. The neural differentiation of the MSCs was induced under the following conditions: before electrical stimulation treatment, all of the cells were cultured under normal culture conditions for 72 h, and the normal culture medium of the MSCs was replaced by the stimulation medium, which contained L-DMEM supplemented with 1% FBS, 1% penicillin–streptomycin, and 20 ng/mL bFGF. The TENG electrical signals were forced at 3000 pulses/day for another 21 days, and the TENG was triggered by human walking with a frequency of about 120 times/min. The culture medium was replaced every 2 days.

Cell Viability Assay. MSCs were seeded on the rGO microfiber and 15% rGO–PEDOT hybrid microfiber. After the cells were cultured under normal conditions for 72 h, a cell viability assay was performed using a live/dead cell imaging kit for mammalian cells (Life Technology) according to the manufacturer’s instructions. A cell counting kit-8 (CCK-8, Dojindo Molecular Technology) was used to quantitatively evaluate cell viability on rGO microfibers and 15% rGO–PEDOT microfibers after cultivation for 1, 3, and 5 days. Ten milligrams of microfibers was placed in a 24-well plate. After MSCs were seeded on the microfibers for certain times, the microfibers were moved to a new 96-well plate and filled with 100 μ L of serum-free L-DMEM medium plus 40 μ L of CCK-8 solution per well. After a 6 h incubation at 37 °C, the resultant production of water-soluble formazan dye was assayed at a wavelength of 450 nm by a microplate reader (MULTISKAN MK3, Thermo, USA). Three parallel replicates for each sample were used.

Immunofluorescence. To investigate the cell adhesion on rGO microfibers and 15% rGO–PEDOT hybrid microfibers, the MSCs on the microfibers were stained with F-actin after 72 h of normal culture. Briefly, the cells were washed with 1 \times PBS, fixed with 4% paraformaldehyde solution in PBS for 20 min, extracted with 0.1% Triton X-100 (Sigma) for 5 min, and blocked with 1% bovine serum albumin (Sigma) for 60 min. The cellular actin filaments were then stained with phalloidin conjugated to AlexaFluor 488 (Invitrogen) at a 1:200 dilution for 120 min, and the nuclei were stained with 4’ 6-diamidino-2-phenylindole (DAPI, 300 nM, Life Technology) for 10 min. The cells were washed three times with 1 \times PBS after each step. After being stimulated by the TENG for another 21 days under the

neural differentiation conditions, the microfibers with the cells were washed with 1 \times PBS, fixed in 4% paraformaldehyde for 20 min, extracted with 0.1% Triton X-100 (Sigma) for 5 min, and blocked with 10% goat serum (Sigma) for 2 h. The samples were incubated with the primary antibodies overnight at 4 °C and then incubated for 2 h at room temperature with the secondary antibodies, followed by DAPI staining. The primary antibody panel included rabbit anti-Tuj1 (1:1000, Abcam) and mouse anti-gliial fibrillary acidic protein (GFAP) (1:1000, Abcam) antibodies. The secondary antibodies were Cy3-conjugated goat anti-rabbit IgG (1:200, Jackson ImmunoResearch) and AlexaFluor 488-conjugated goat anti-mouse IgG (1:200, Jackson ImmunoResearch). Finally, the cells were imaged with a Leica confocal microscope SP8, and the 3D scanning immunofluorescence micrographs were captured with CLSM in a z-stack model.

qPCR. Neural differentiation of MSCs on rGO microfibers and 15% rGO–PEDOT hybrid microfibers was performed by assessment of the gene expressions using qPCR at day 21 under TENG electrical stimulation conditions. The total RNA was extracted from the cells using the RNeasy Plus Mini Kit (Qiagen) according to the manufacturer’s instructions. The RNA samples were reverse-transcribed into cDNA for qPCR using the PrimeScriptTM reagent kit with gDNA Eraser (Takara). qPCR was performed with SYBR Premix Ex TaqTM with ROX (Takara) according to the manufacturer’s instructions. The signals were detected with an ABI 7500 Fast real time PCR system (Applied Biosystems) to analyze the expressions of Tuj1 and GFAP. The gene expression was normalized to glyceraldehyde-3-phosphate dehydrogenase (GAPDH) as the internal standard. Information on the primers is provided in Supporting Information Table S1.

Statistical Analysis. The data were reported as the mean \pm SD, and statistical analysis was performed using the unpaired Student’s *t* test. Statistical significance was accepted at **p* \leq 0.05 and ***p* \leq 0.01.

ASSOCIATED CONTENT

Supporting Information

The Supporting Information is available free of charge on the ACS Publications website at DOI: 10.1021/acsnano.6b00200.

Images, Raman spectra, FTIR characterizations, adsorption of proteins, biodegradability, MSCs purity, MSCs on graphene film and primers sequences (PDF)

Movie S1 (AVI)

Movie S2 (AVI)

AUTHOR INFORMATION

Corresponding Authors

*E-mail: lilinlin@binn.cas.cn.

*E-mail: hongliu@sdu.edu.cn.

*E-mail: zlwang@binn.cas.cn.

Notes

The authors declare no competing financial interest.

ACKNOWLEDGMENTS

The authors are thankful for funding from the National Natural Science Foundation of China (Grant Nos. 51402063, 31270022, and 81471784), the China Postdoctoral Science Foundation (No. 2014M550673), the Fundamental Research Funds of Shandong University (2014QY003), and the “100 Talents Program” of the Chinese Academy of Sciences. Thanks are also due to support from the “Thousands Talents” program for pioneer researchers and his innovation team, China.

REFERENCES

(1) Schmidt, C. E.; Leach, J. B. Neural Tissue Engineering: Strategies for Repair and Regeneration. *Annu. Rev. Biomed. Eng.* **2003**, *5*, 293–347.

- (2) Willerth, S. M.; Sakiyama-Elbert, S. E. Approaches to Neural Tissue Engineering Using Scaffolds for Drug Delivery. *Adv. Drug Delivery Rev.* **2007**, *59*, 325–338.
- (3) Bianco, P.; Robey, P. G. Stem Cells in Tissue Engineering. *Nature* **2001**, *414*, 118–121.
- (4) Toma, C.; Pittenger, M. F.; Cahill, K. S.; Byrne, B. J.; Kessler, P. D. Human Mesenchymal Stem Cells Differentiate to a Cardiomyocyte Phenotype in the Adult Murine Heart. *Circulation* **2002**, *105*, 93–98.
- (5) Aurich, I.; Mueller, L. P.; Aurich, H.; Luetzkendorf, J.; Tisljar, K.; Dollinger, M. M.; Schormann, W.; Walldorf, J.; Hengstler, J. G.; Fleig, W. E.; et al. Functional Integration of Hepatocytes Derived from Human Mesenchymal Stem Cells into Mouse Livers. *Gut* **2007**, *56*, 405–415.
- (6) Takashima, Y.; Era, T.; Nakao, K.; Kondo, S.; Kasuga, M.; Smith, A. G.; Nishikawa, S. I. Neuroepithelial Cells Supply an Initial Transient Wave of MSC Differentiation. *Cell* **2007**, *129*, 1377–1388.
- (7) Wislet-Gendebien, S.; Hans, G.; Leprince, P.; Rigo, J. M.; Moonen, G.; Rogister, B. Plasticity of Cultured Mesenchymal Stem Cells: Switch from Nestin-Positive to Excitable Neuron-Like Phenotype. *Stem Cells* **2005**, *23*, 392–402.
- (8) Phinney, D. G.; Prockop, D. J. Concise review: Mesenchymal Stem/Multipotent Stromal Cells: The State of Transdifferentiation and Modes of Tissue Repair-Current Views. *Stem Cells* **2007**, *25*, 2896–2902.
- (9) Subramanian, A.; Krishnan, U. M.; Sethuraman, S. Development of Biomaterial Scaffold for Nerve Tissue Engineering: Biomaterial Mediated Neural Regeneration. *J. Biomed. Sci.* **2009**, *16*, 108.
- (10) Zhang, Y.; Nayak, T. R.; Hong, H.; Cai, W. Graphene: a Versatile Nanoplatforform for Biomedical Applications. *Nanoscale* **2012**, *4*, 3833–3842.
- (11) Kim, J.; Kim, Y. R.; Kim, Y.; Lim, K. T.; Seonwoo, H.; Park, S.; Cho, S. P.; Hong, B. H.; Choung, P. H.; Chung, T. D. Graphene-Incorporated Chitosan Substrata for Adhesion and Differentiation of Human Mesenchymal Stem Cells. *J. Mater. Chem. B* **2013**, *1*, 933–938.
- (12) Sanchez, V. C.; Jachak, A.; Hurt, R. H.; Kane, A. B. Biological Interactions of Graphene-Family Nanomaterials: an Interdisciplinary Review. *Chem. Res. Toxicol.* **2012**, *25*, 15–34.
- (13) Kalbacova, M.; Broz, A.; Kong, J.; Kalbac, M. Graphene Substrates Promote Adherence of Human Osteoblasts and Mesenchymal Stromal Cells. *Carbon* **2010**, *48*, 4323–4329.
- (14) Mao, H. Y.; Laurent, S.; Chen, W.; Akhavan, O.; Imani, M.; Ashkarran, A. A.; Mahmoudi, M. Graphene: Promises, Facts, Opportunities, and Challenges in Nanomedicine. *Chem. Rev.* **2013**, *113*, 3407–3424.
- (15) Bitounis, D.; Ali-Boucetta, H.; Hong, B. H.; Min, D. H.; Kostarelos, K. Prospects and Challenges of Graphene in Biomedical Applications. *Adv. Mater.* **2013**, *25*, 2258–2268.
- (16) Tan, X.; Feng, L.; Zhang, J.; Yang, K.; Zhang, S.; Liu, Z.; Peng, R. Functionalization of Graphene Oxide Generates a Unique Interface for Selective Serum Protein Interactions. *ACS Appl. Mater. Interfaces* **2013**, *5*, 1370–1377.
- (17) Kim, D. H.; Richardson-Burns, S. M.; Hendricks, J. L.; Sequera, C.; Martin, D. C. Effect of Immobilized Nerve Growth Factor on Conductive Polymers: Electrical Properties and Cellular Response. *Adv. Funct. Mater.* **2007**, *17*, 79–86.
- (18) Richardson-Burns, S. M.; Hendricks, J. L.; Foster, B.; Povlich, L. K.; Kim, D. H.; Martin, D. C. Polymerization of the Conducting Polymer Poly (3, 4-ethylenedioxythiophene) (PEDOT) Around Living Neural Cells. *Biomaterials* **2007**, *28*, 1539–1552.
- (19) Gkoupidenis, P.; Schaefer, N.; Garlan, B.; Malliaras, G. G. Neuromorphic Functions in PEDOT: PSS Organic Electrochemical Transistors. *Adv. Mater.* **2015**, *27*, 7176–7180.
- (20) Weaver, C. L.; Cui, X. T. Directed Neural Stem Cell Differentiation with a Functionalized Graphene Oxide Nanocomposite. *Adv. Healthcare Mater.* **2015**, *4*, 1408–1416.
- (21) Ghasemi-Mobarakeh, L.; Prabhakaran, M. P.; Morshed, M.; Nasr-Esfahani, M. H.; Baharvand, H.; Kiani, S.; Al-Deyab, S. S.; Ramakrishna, S. Application of Conductive Polymers, Scaffolds and Electrical Stimulation for Nerve Tissue Engineering. *J. Tissue Eng. Regen. Med.* **2011**, *5*, e17–e35.
- (22) Tang, M.; Song, Q.; Li, N.; Jiang, Z.; Huang, R.; Cheng, G. Enhancement of Electrical Signaling in Neural Networks on Graphene Films. *Biomaterials* **2013**, *34*, 6402–6411.
- (23) Heo, C.; Yoo, J.; Lee, S.; Jo, A.; Jung, S.; Yoo, H.; Lee, Y. H.; Suh, M. The Control of Neural Cell-to-Cell Interactions Through Non-Contact Electrical Field Stimulation Using Graphene Electrodes. *Biomaterials* **2011**, *32*, 19–27.
- (24) Zhu, G.; Bai, P.; Chen, J.; Wang, Z. L. Power-Generating Shoe Insole Based on Triboelectric Nanogenerators for Self-Powered Consumer Electronics. *Nano Energy* **2013**, *2*, 688–692.
- (25) Zi, Y.; Niu, S.; Wang, J.; Wen, Z.; Tang, W.; Wang, Z. L. Standards and Figure-of-Merits for Quantifying the Performance of Triboelectric Nanogenerators. *Nat. Commun.* **2015**, *6*, 8376.
- (26) Yu, X.; Han, X.; Zhao, Z.; Zhang, J.; Guo, W.; Pan, C.; Li, A.; Liu, H.; Wang, Z. L. Hierarchical TiO₂ Nanowire/Graphite Fiber Photoelectrocatalysis Setup Powered by a Wind-Driven Nanogenerator: A Highly Efficient Photoelectrocatalytic Device Entirely Based on Renewable Energy. *Nano Energy* **2015**, *11*, 19–27.
- (27) Han, C. B.; Jiang, T.; Zhang, C.; Li, X.; Zhang, C.; Cao, X.; Wang, Z. L. Removal of Particulate Matter Emissions from Vehicle Using a Self-Powered Triboelectric Filter. *ACS Nano* **2015**, *9*, 12552–12561.
- (28) Zheng, Q.; Shi, B.; Fan, F.; Wang, X.; Yan, L.; Yuan, W.; Wang, S.; Liu, H.; Li, Z.; Wang, Z. L. *In Vivo* Powering of Pacemaker by Breathing-Driven Implanted Triboelectric Nanogenerator. *Adv. Mater.* **2014**, *26*, 5851–5856.
- (29) Pu, X.; Li, L.; Song, H.; Du, C.; Zhao, Z.; Jiang, C.; Cao, G.; Hu, W.; Wang, Z. L. A Self-Charging Power Unit by Integration of a Textile Triboelectric Nanogenerator and a Flexible Lithium-Ion Battery for Wearable Electronics. *Adv. Mater.* **2015**, *27*, 2472–2478.
- (30) Dong, Z.; Jiang, C.; Cheng, H.; Zhao, Y.; Shi, G.; Jiang, L.; Qu, L. Facile Fabrication of Light, Flexible and Multifunctional Graphene Fibers. *Adv. Mater.* **2012**, *24*, 1856–61.
- (31) Luo, X.; Weaver, C. L.; Tan, S.; Cui, X. T. Pure Graphene Oxide Doped Conducting Polymer Nanocomposite for Bio-interfacing. *J. Mater. Chem. B* **2013**, *1*, 1340–1348.
- (32) Park, S. Y.; Park, J.; Sim, S. H.; Sung, M. G.; Kim, K. S.; Hong, B. H.; Hong, S. Enhanced Differentiation of Human Neural Stem Cells into Neurons on Graphene. *Adv. Mater.* **2011**, *23*, H263–H267.
- (33) Park, S.; Mohanty, N.; Suk, J. W.; Nagaraja, A.; An, J.; Piner, R. D.; Cai, W.; Dreyer, D. R.; Berry, V.; Ruoff, R. S. Biocompatible, Robust Free-Standing Paper Composed of a TWEEN/Graphene Composite. *Adv. Mater.* **2010**, *22*, 1736–1740.
- (34) Shi, X.; Chang, H.; Chen, S.; Lai, C.; Khademhosseini, A.; Wu, H. Regulating Cellular Behavior on Few-Layer Reduced Graphene Oxide Films with Well-Controlled Reduction States. *Adv. Funct. Mater.* **2012**, *22*, 751–759.
- (35) Guo, W.; Wang, S.; Yu, X.; Qiu, J.; Li, J.; Tang, W.; Li, Z.; Mou, X.; Liu, H.; Wang, Z. Construction of a 3D rGO-Collagen Hybrid Scaffold for Enhancement of the Neural Differentiation of Mesenchymal Stem Cells. *Nanoscale* **2016**, *8*, 1897–1904.
- (36) Kotchey, G. P.; Allen, B. L.; Vedala, H.; Yanamala, N.; Kapralov, A. A.; Tyurina, Y. Y.; Klein-Seetharaman, J.; Kagan, V. E.; Star, A. The Enzymatic Oxidation of Graphene Oxide. *ACS Nano* **2011**, *5*, 2098–2108.
- (37) Li, Y.; Feng, L.; Shi, X.; Wang, X.; Yang, Y.; Yang, K.; Liu, T.; Yang, G.; Liu, Z. Surface Coating-Dependent Cytotoxicity and Degradation of Graphene Derivatives: Towards the Design of Non-Toxic, Degradable Nano-Graphene. *Small* **2014**, *10*, 1544–1554.
- (38) Chen, G. Y.; Pang, D. P.; Hwang, S. M.; Tuan, H. Y.; Hu, Y. C. A Graphene-Based Platform for Induced Pluripotent Stem Cells Culture and Differentiation. *Biomaterials* **2012**, *33*, 418–427.
- (39) Tang, W.; Tian, J.; Zheng, Q.; Yan, L.; Wang, J.; Li, Z.; Wang, Z. L. Implantable Self-Powered Low-Level Laser Cure System for Mouse Embryonic Osteoblasts' Proliferation and Differentiation. *ACS Nano* **2015**, *9*, 7867–7873.

(40) Zhu, G.; Chen, J.; Zhang, T.; Jing, Q.; Wang, Z. L. Radial-Arrayed Rotary Electrification for High Performance Triboelectric Generator. *Nat. Commun.* **2014**, *5*, 3426.

(41) Li, N.; Zhang, Q.; Gao, S.; Song, Q.; Huang, R.; Wang, L.; Liu, L.; Dai, J.; Tang, M.; Cheng, G. Three-Dimensional Graphene Foam As a Biocompatible and Conductive Scaffold for Neural Stem Cells. *Sci. Rep.* **2013**, *3*, 1604.

(42) Shah, S.; Yin, P. T.; Uehara, T. M.; Chueng, S. T. D.; Yang, L.; Lee, K. B. Guiding Stem Cell Differentiation into Oligodendrocytes Using Graphene-Nanofiber Hybrid Scaffolds. *Adv. Mater.* **2014**, *26*, 3673–3680.

(43) Gage, F. H.; Temple, S. Neural Stem Cells: Generating and Regenerating the Brain. *Neuron* **2013**, *80*, 588–601.

(44) Zhang, H.; Lv, X.; Li, Y.; Wang, Y.; Li, J. P25-Graphene Composite As a High Performance Photocatalyst. *ACS Nano* **2010**, *4*, 380–386.